JOURNAL OF NEUROTRAUMA 33:354–361 (February 15, 2016)

DOI: 10.1089/neu.2015.3913

Transition from Initial Hypoactivity to Hyperactivity in Cortical Layer V Pyramidal Neurons after Traumatic Brain Injury *In Vivo*

Xingjie Ping and Xiaoming Jin

Abstract

Traumatic brain injury (TBI) often results in structural damage and a loss of neurons that is commonly accompanied by early changes in neuronal electrical activity. Loss of neuronal activity has been hypothesized to contribute to post-traumatic epileptogenesis through the regulation of homeostatic plasticity. The existence of activity loss in cortical neurons after TBI and its subsequent transition into hyperactivity over time is not well characterized, however, particularly in models of TBI *in vivo*. In the current study, changes in neuronal activity in the primary motor cortex after moderate controlled cortical impact (CCI) in mice were studied using a single-unit recording technique *in vivo*. Recordings were made at different time points after CCI from cortical layer V pyramidal neurons that were within 1–2 mm from the anterior edge of the injured foci. Within 1–4 h after CCI, the frequency of spontaneous single-unit activity depressed significantly, with the mean firing frequency decreasing from 2.59 ± 0.18 Hz in the sham group to 1.05 ± 0.20 Hz of the injured group. The firing frequencies recovered to the normal level at 1 day and 7 days post-CCI, but became significantly higher at 3 days and 14 days post-CCI. The results suggest that TBI caused initial loss of activity in neurons of the perilesional cortical region, which was followed by compensatory recovery and enhancement of activity. These time-dependent changes in neuronal activity may contribute to the development of hyperexcitability through homeostatic activity regulation.

Key words: action potential; neuronal activity; post-traumatic epilepsy; single-unit recording; traumatic brain injury

Introduction

Traumatic brain injury (TBI) often results in structural damage and neuronal loss that is commonly accompanied by immediate changes in the pattern and level of neuronal activity. An early decrease in neuronal activity has been documented as depressed excitatory transmission and network activity after injury in acute slice or organotypic slice culture,[1,2] as reduced action potential firing or multiunit activity in models of TBI in rats or cats,[3,4] and as reduced spontaneous multiunit activity and suppressed evoked potential in patients with TBI.[3,5] Similarly, reductions in action potential firing and evoked potentials occur in neurons of the peri-infarct region immediately after ischemic stroke, and last for hours to days.[6–8]

Loss of neuronal activity after TBI has been hypothesized to activate homeostatic regulation of activity and contribute to the development of post-traumatic epilepsy, a severe neurological condition featuring synchronized paroxysmal activity of the surviving neurons in the injured brain regions.[9,10] The homeostatic plasticity mechanism is well established in the developing cortex and recently in the adult cortex, in which neuronal excitability and synaptic activity in cortical neurons can scale up or down to compensate for a decrease or increase in action potential firing rate, respectively.[11–14] For example, chronic blockade of action potential firing by tetrodotoxin induces homeostatic plasticity that involves changes in excitatory and inhibitory synaptic transmission and spontaneous seizures on removal of the activity blockade in the hippocampus *in vitro*[15,16] or *in vivo*.[13] Chronic partial denervation by cutting Schaffer collaterals of the hippocampus leads to a delayed homeostatic increase in neuronal excitability.[17] In the partially isolated neocortex (undercut) model of post-traumatic epileptogenesis,[18–20] the deafferented neocortical region exhibits long periods of silence and brief bursts of activity and subsequent development of paroxysmal discharge.[4,21] These studies indicate that loss of activity may be an initial factor that eventually leads to post-traumatic epileptogenesis.

Characterizing activity loss after TBI is the first step toward establishing the potential role of homeostatic regulation in post-traumatic epileptogenesis. Because most previous electrophysiological studies on TBI focused on measuring neuronal activity and network excitability at a single time point, however, changes in neuronal activity over a time period post-TBI are not understood. Particularly, the duration and severity of such post-injury activity loss *in vivo* is not well characterized. Further, the prominent feature

Department of Anatomy and Cell Biology, Stark Neuroscience Research Institute, Indiana Spinal Cord and Brain Injury Research Group, Indiana University School of Medicine, Indianapolis, Indiana.

of deafferentation in the models of undercut and hippocampal lesion discussed above are not commonly seen in other animal models and typical cases of TBI, which leads to the question about whether homeostatic regulation hypothesis is also involved in post-traumatic epileptogenesis in other contusive models of TBI.

Therefore, we used *in vivo* extracellular single-unit recording to monitor action potential firing in mouse neocortex at different times after controlled cortical impact (CCI), a widely used animal model of TBI in which post-traumatic epileptogenesis has been established by several groups.[22–24] Because of the roles of cortical layer V in initiating epileptiform activities[20,25] and our previous work on the neurophysiology of pyramidal neurons and interneurons in layer V,[26–28] we continued focusing on this population of neurons. Our results showed time-dependent changes in neuronal activity after TBI that involved early hypoactivity after injury and a later hyperactivity at 2 weeks after TBI.

Methods

Animals

Male C57BL6 mice aged 2 months old were used for this experiment. The mice were kept in our animal facility on a 12-hour light/dark cycle, with food and water supplied *ad libitum*. All procedures were approved by the Animal Care and Use Committee of the Institutional Guide for the Care and Use of Laboratory Animals at Indiana University School of Medicine.

Controlled cortical impact model of TBI

The mice were anesthetized with intraperitoneal ketamine/xylazine (87.7/12.3 mg/kg) and were fixed on a stereotaxic apparatus. After a midline incision on the scalp, a ~4 mm craniotomy was performed above the left hemisphere of the brain, with the center being between the lambda and bregma sutures of the skull and the medial edge being 1 mm from the midline. An Impact One™ stereotaxic impactor (Leica Microsystems Inc., Buffalo Grove, IL) with a 3-mm diameter rod tip was used to compress the cortex at a velocity of 3.0 m/sec to a depth of 1.0 mm. This setting allowed us to generate moderate TBI of the brain. A small piece of sterile plastic film was used to cover the burr hole, and the scalp was sutured. The mice in the sham group received only the craniotomy without cortical impact.

Because TBI-induced brain edema may increase cortical thickness, we also measured changes in cortical thickness in 12 mice (2 in each group). The mice were sacrificed after sham injury or at 1–4 h, 1 day, 3 days, 7 days, and 14 days after CCI, respectively. Fresh coronal slices across the level of the recording site were cut immediately with a vibratome and imaged using a digital CCD camera (Fig. 1D–F). Thicknesses of the ipsilateral and contralateral cortex were measured and the percentage of cortical swelling was calculated by dividing the ipsilateral cortical thickness by contralateral cortical thickness.

Single-unit recording

Extracellular single-unit recordings were made from the primary motor cortex of the mice within 1–4 h, or at 1, 3, 7, or 14 days after CCI. Before the recording, the animal was anesthetized with intraperitoneal ketamine/xylazine (87.7/12.3 mg/kg)[29] and placed in a stereotaxic apparatus with a heating patch under its body to keep it warm. A 1.5–2 mm diameter hole was drilled on the skull for inserting a recording electrode. The hole was located 1-mm lateral to the midline and 1–2 mm from the anterior edge of the cranial window that had been used to create for CCI (Fig. 1A). Recording electrodes were pulled from borosilicate glass tubing (impedance of 8–12 MΩ) and filled with 2 M NaCl solution. The recording electrode was mounted on a motorized micromanipulator (PatchStar, Scientifica, UK), which was calibrated and controlled by software.

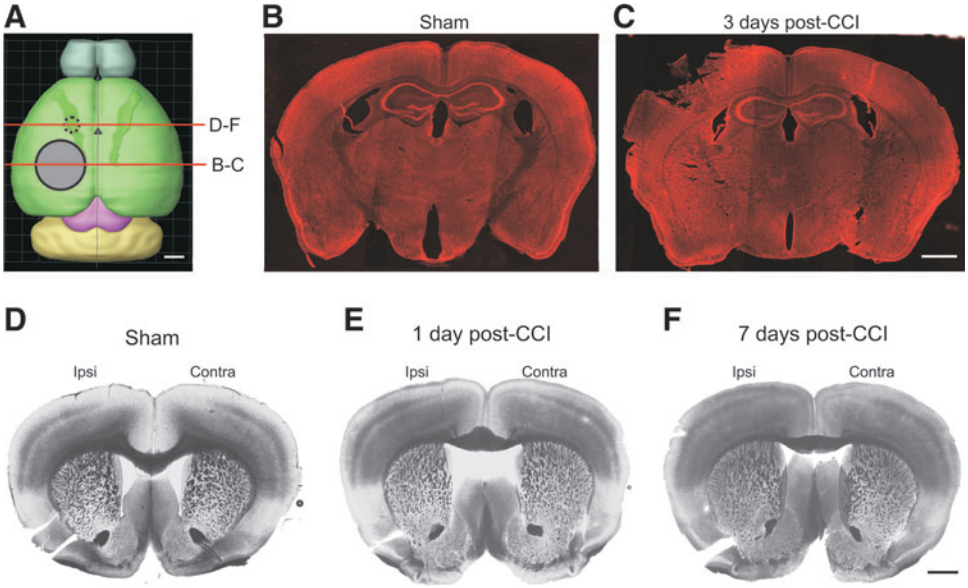

FIG. 1. *In vivo* single-unit recording from control and injured primary motor cortex in mice. (**A**) Top view of a whole mouse brain showing the locations of controlled cortical impact (CCI, large grey circle), recording site (small dotted circle), and the surface projection of the primary motor cortex (bright green area). The black triangle indicates bregma; the two red lines indicate corresponding levels of coronal sections in the following images (B–F). (**B,C**) Fluorescent Nissl staining of coronal cortical slices of the sham and CCI-injured brains. There are tissue loss and damage from superficial to deep cortical layers at 3 days post-CCI (C). (**D–F**) Unfixed brain slices across the level of *in vivo* cortical recording site after sham injury, and at 1 and 7 days after CCI. The differences in cortical thickness between ipsilateral (Ipsi) and contralateral (Contra) hemispheres are small in these sections. Scale bars: 1 mm in all images. The mouse brain image was created with Allen Mouse Brain Atlas using Brain Explorer® 2 (Website: ©2014 Allen Institute for Brain Science. Allen Mouse Brain Atlas: http://mouse.brain-map.org/). Color image is available online at www.liebertpub.com/neu

The position and orientation of the mouse head was carefully adjusted so that the cortical surface of the recorded hemisphere was perpendicular to the recording electrode. The recording electrode was then vertically lowered through the dura into the neocortex. Under continuous monitoring of spontaneous activity, the pipette was firstly inserted to $\sim 400\,\mu$m below the pial surface and then slowly advanced at 5 μm until a single-unit activity was clearly detected and remained stable. After a 3–5 min waiting period for the spontaneous firing to become stable, recordings were made and lasted for 10–15 min. During each recording session, the exposed cortex was covered by a small piece of saline cotton to keep the tissue from drying.

Because the level of anesthesia affects the rate of spontaneous firing, it is important that *in vivo* recordings were made when the animals were in a stable state of anesthesia. To determine the duration and depth of anesthesia after ketamine/xylazine injection, we monitored mouse response to tail pinch, heart rate, blood pressure, and electroencephalography (EEG) in four control mice. We found that the mice maintained a stable blood pressure and EEG frequency patterns for 25–30 min after initial or supplemental (at ½ dosage) injection of ketamine/xylazine. Their responsiveness to tail pinch was closely correlated with increase in blood pressure, suggesting that the mice were awakening from the anesthesia state.

These observations were consistent with previous studies showing that ketamine-induced anesthesia lasted for about 30 min, during which stable EEG patterns are maintained and cortical neurons have depressed but constant firing activity.[30,31] Therefore, our recordings were made in a time window between 5–25 min after initial or supplemental drug injection, during which the response to tail pinch and breath rate were monitored.

Signals were filtered (~ 10 kHz) and recorded with MultiClamp 700B (Molecular Devices, Sunnyvale, CA) and were saved in a computer. At the end of the experiment, the mice were sacrificed with a lethal injection of sodium pentobarbital.

Histological verification of recording sites

We used the depths of pipette penetration driven by the micromanipulator to measure the depths of the recorded neurons and their laminar location in the cortex.[32,33] This approach allowed us to efficiently record multiple neurons from a mouse, but there might be a deviation between the anatomical location of a recorded neuron and the penetration depth of the recording electrode. To correct this error, we compared the anatomical locations of pipette tips marked by electrocoagulation and the depth of pipette penetration in a subset of recorded mice ($n = 10$).

After a glass micropipette was lowered into the cortex, the depth of penetration relative to the pial surface was recorded, and a recording was made. A single current (600 μA, 200 μs) was applied with an isolated pulse stimulator (Model 2100, A-M systems, Sequim, WA) through the pipette. Animals were then sacrificed, and the brains were removed. The cortical regions containing the recording sites were sectioned at a thickness of 200 μm using a vibratome (Leica VT1200, Leica Biosystems, Richmond, IL). The unfixed brain slices were immediately observed under a microscope (Zeiss Axio Imager M2), and images were captured using a digital CCD camera.

Nissl staining

Mice receiving CCI or sham injury were deeply anesthetized and then were perfused transcardially with 0.9% NaCl followed by 4% paraformaldehyde. The brains were removed, postfixed overnight, and transferred to a 30% sucrose solution until they sank. The brains were sectioned at 30 μm using the Leica CM1950 cryostat. The sections were rehydrated in 0.01 M phosphate-buffered saline (PBS, pH 7.2) for 40 min, followed by washing in PBS plus 0.1% Triton® X-100 for 10 min. After two washes in PBS, the sections were then incubated with NeuroTrace solution (1:200 in PBS, Life Technologies, Grand Island, NY) for 20 min at room temperature. After several washes at room temperature, the sections were mounted with FluoroGel mounting medium (GeneTex, Irvine, CA) and were imaged with an inverted microscope system (Zeiss, Axiovert 200M equipped with Apotome).

Data analysis

Single units were automatically detected based on rise time, amplitude, and duration of the events using Wdetecta software.[27] The detecting parameters were manually adjusted for each recording trace to ensure correct detection of all single units. By overlaying individual spikes at the beginning, the middle, and the end of each trace, we confirmed that the waveform of each single unit was generally constant during the recording period (Fig. 3A,B inserts). Recordings with increasing spike width during the recording period were excluded from the data analysis. Based on published studies, pyramidal neurons were identified using the following criteria: (1) the mean firing frequency of the spike was lower than 10 Hz; (2) the spike width was longer than 660 μs.[34,35]

Statistical analyses of spike frequency were performed using GraphPad Prism 5.0 software. Data were presented as mean ± standard error of the mean. Statistical comparisons of cortical depth and firing frequency among all groups were made using one-way analysis of variance (ANOVA) followed by Newman-Keuls multiple comparison test. Distribution of fractions of events with different interspike intervals (ISI) among all groups was analyzed with two-way ANOVA followed by the Bonferroni *post hoc* test. The percent of events with ISI ≤10 msec was compared with the Mann-Whitney *U* test. The statistical significance was set at $p < 0.05$.

Results

Extracellular single-unit recordings were made from a total of 165 neurons in the primary motor cortex from 48 adult mice of the sham and injured groups. The number of mice in each group and the number of recorded neurons from each mouse are listed in Table 1. Recordings were made consistently from a small area that was 1–2 mm anterior and parallel to the medial edge of the CCI lesion site or a homotopic area of sham injured cortex (Fig. 1A). Moderate TBI induced by CCI resulted in a partial loss of cortical tissue, as was revealed in coronal sections using fluorescent Nissl staining (Fig. 1B,C).

The depths of electrode penetration relative to the pial surface at each recording site were used to estimate the location of the recorded neurons. We verified the accuracy of this method for neuronal localization by comparing the penetration depths of the recording electrodes and the anatomical distances between the recorded neurons as marked by electrical currents and the pia in fresh coronal sections. The mean measured pipette tip location was $52.8 \pm 7.5\,\mu$m deeper than the penetration depth from micromanipulator movement. Therefore, the depths of the neurons recorded were corrected by adding this average value.

We also found slight increases in cortical thickness after CCI. The thicknesses of the ipsilateral cortex were 100%, 100.3%, 103.7%, 105.6%, 103.45, and 102.7% of the contralateral cortex in the sham, and 1–4 h, and 1, 3, 7, and 14 days post-CCI groups, respectively (Fig. 1D–F). The measured cortical depth of each neuron was further adjusted. Neurons that were located within 500–800 μm below the pial surface were classified as layer V pyramidal neurons and included in data analysis. Locations of the neurons were also confirmed in Nissl staining sections (Fig. 2A). The average depths of the recorded cortical neurons were similar among all the five groups ($p > 0.05$, One-way ANOVA, Fig. 2B).

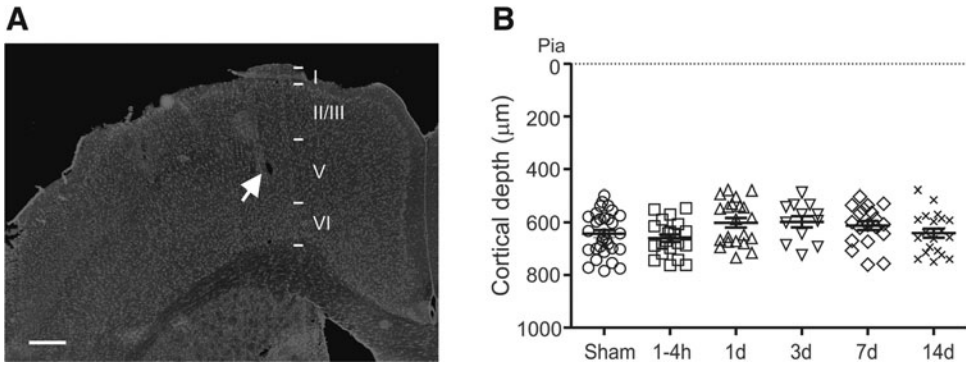

FIG. 2. Locations of recording pipettes within the neocortex. (**A**) A representative image of Nissl staining shows the location of the tip of a recording pipette in layer V of the cortex (white arrow), which was made by applying an electric current (1 mA, 200 μsec) to the electrode at the end of recordings. (**B**) Distributions of the depth of the recorded cortical neurons in each group. Each dot in the graph represents the location of a neuron relative to the pial surface. There were no significant differences in the mean depths among all groups ($p > 0.05$, one-way analysis of variance). Scale bar in A: 250 μm.

We analyzed the firing frequencies in cortical layer V pyramidal neurons, which accounted for the majority of the recorded neurons (82% of the 165 neurons recorded). To determine whether there was any difference at different times after sham injury, we made recordings from mice at 1–4 h and 14 days after sham injury. The firing rates of layer V pyramidal neurons in these two sham groups were very close, so the data were pooled as a single sham group. In the sham group, the mean frequency of spontaneous single-unit activity was 2.59 ± 0.18 Hz ($n = 31$).

The CCI caused significant changes in the frequencies of spontaneous activity of these neurons at different post-injury times (Fig. 3,4). Within 1–4 h after CCI, the firing frequency of the layer V pyramidal neurons became significantly lower than the sham group (1.05 ± 0.20 Hz, $n = 21$, $p < 0.01$, One-way ANOVA followed by Newman-Keuls multiple comparison test. Fig. 3A,B and Fig. 4). This depressed activity was followed by a recovery of firing frequency at 1 day post-CCI (2.34 ± 0.39 Hz, $n = 21$), which was higher than 1–4 h post-CCI (Fig. 4, $p < 0.05$); then an overshoot at 3 days post-CCI (3.87 ± 0.67 Hz, $n = 12$), which was significantly higher than the 1–4 h post-CCI group (Fig. 4, $p < 0.001$).

At 7 days post-CCI, the firing frequency recovered to about the level of the sham group level (2.49 ± 0.70 Hz, $n = 16$) and higher than the 1–4 h post-CCI group ($p < 0.05$). At 14 days post-CCI, the frequency again became significantly higher (4.30 ± 0.43 Hz, $n = 20$) than the sham ($p < 0.01$) and 1–4 h ($p < 0.001$), 1 day ($p < 0.01$), and 7 days post-CCI groups ($p < 0.05$) (Fig. 4), suggesting a state of neuronal hyperactivity.

To determine potential changes in the pattern of neuronal firing, we further plotted histograms to determine the distribution of inter-spike interval (ISI) of each group. In the sham group, events with <0.1 sec ISI accounted for about 40% of the total number of events, and events with ISI between 0.1–1.6 sec accounted for most of the remaining percentage (Fig. 5A). The fraction of events with ISI <0.1 sec in the 1–4 h post-CCI group became lower than the sham group and all the other CCI groups ($p < 0.001$, two-way ANOVA followed by the Bonferroni *post hoc* test), but the fraction of these events in 3 and 14 day post-CCI group became higher than the 1 day post-CCI group ($p < 0.001$, two-way ANOVA followed by the Bonferroni *post hoc* test).

In contrast, the fraction of events with ISI between 0.4–0.8 sec in the 7 day post-CCI group was significantly lower than the sham, and 1–4 h and 1 day post-CCI groups (Fig. 5A). The results indicate that events with less than 0.1 sec ISI accounted for the majority of the total spontaneous events and that the trends of their increase or decrease at different times after TBI were generally consistent with the mean firing frequencies of all groups.

In animal models of chronic epilepsy, previous studies found an increase in the number of burst spiking in hippocampal pyramidal neurons that fire action potentials at more than 100 Hz within a burst.[36,37] Because there are also burst spiking pyramidal neurons in cortical layer V,[38,39] we examined the percentage of events with ISI ≤10 msec in each neuron to determine their burst firing activity. The percentages of events with ISI ≤10 msec in 1–4 h and 1 day post-CCI groups were significantly lower than the sham group and almost all other CCI groups. (Fig. 5B, $p < 0.05 - p < 0.01$, one-way ANOVA followed by the Bonferroni *post hoc* test). The result suggested an acute decrease in burst firing activity in these neurons after TBI.

Discussion

Neuronal activity is essential for normal brain functions. It plays a key role in guiding and sculpting circuit formation in the developing

Table 1. Number of Recorded Cell in Each Mouse of all Experimental Groups

Group	*No. of animals*	*No. of neurons*	*No. of neurons from each mouse*
Sham	12	31	1, 2, 3, 2, 4, 3, 2, 3, 2, 3, 2, 4
1–4 hours post-CCI	11	21	1, 1, 1, 3, 4, 1, 1, 3, 2, 3, 1
1 day post-CCI	6	21	2, 3, 2, 5, 4, 5
3 days post-CCI	6	12	2, 2, 2, 2, 2, 2
7 days post-CCI	7	16	2, 2, 2, 3, 3, 1, 3
14 days post-CCI	6	20	4, 4, 3, 3, 4, 2

CCI, controlled cortical impact.

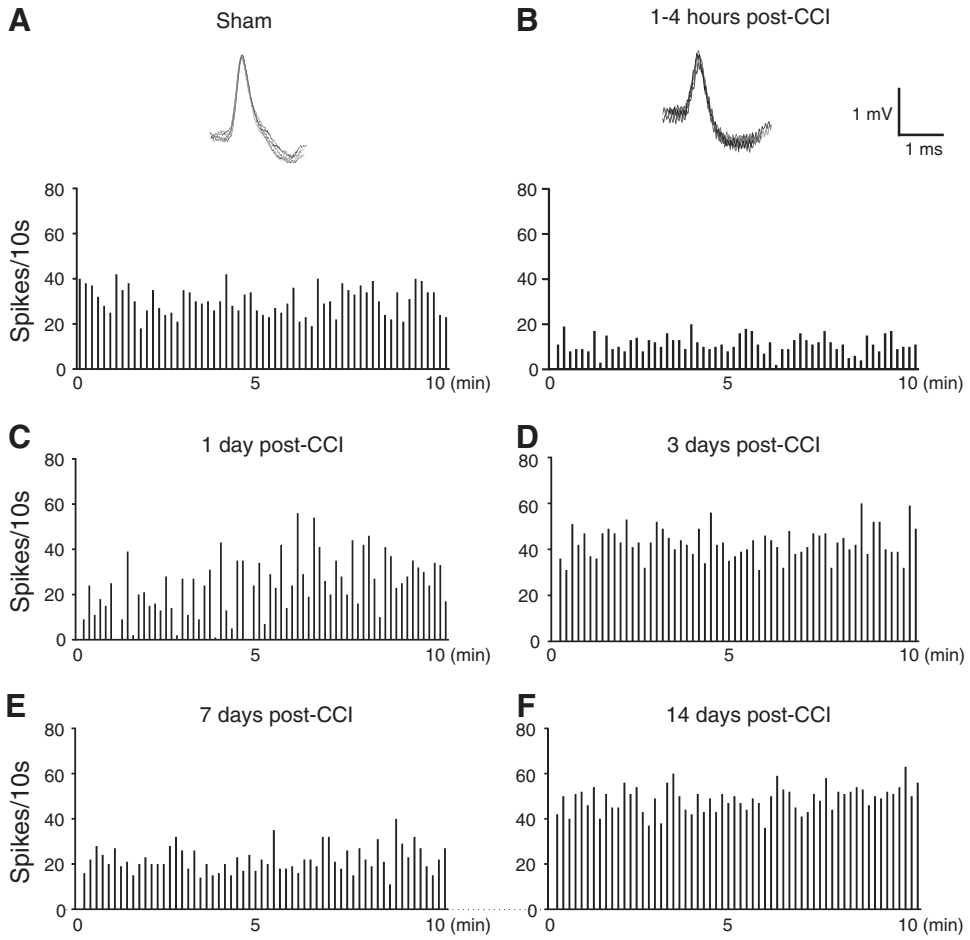

FIG. 3. Single-unit recordings from layer V pyramidal neurons of the sham and injured neocortex *in vivo*. (**A–F**). Representative single-unit recordings made from neurons of the sham-injured group (A), and in 1–4 h (B), and at 1 day (C), 3 days (D), 7 days (E), and 14 days (F) after controlled cortical impact (CCI). In the 10-min recording periods, the time bins in each frequency histogram are 10 sec wide. Note the dramatic decrease in firing rates in a neuron within 1–4 h after CCI and increases in firing rate in neurons at 3 and 14 days after CCI. The inserts in A and B show representative traces of single-unit activity at the beginning, middle, and end of recording; the waveforms of each single-unit activity were consistent throughout the recording period.

brain[40,41] and is likely involved in the plasticity, repair, and epileptogenesis after brain injury as well.[10,42] Understanding neural activity profiles after TBI may shed light on the mechanisms of TBI-induced functional deficits as well as post-traumatic epileptogenesis. In this study, we recorded single-unit activity in cortical layer V pyramidal neurons at different time points after moderate CCI *in vivo*.

Our results showed that CCI resulted in an acute decrease in spontaneous firing rate of these neurons that were adjacent to the foci of TBI injury. This reduced firing was followed by recoveries to nearly normal firing rates at 1 day and 7 days post-CCI but higher firing rates at 3 days and 14 days post-CCI. These time-dependent changes in firing rates revealed that an acute loss of activity after TBI is followed by a trend of homeostatic/compensatory recovery of activity and development of hyperactivity, which may contribute to post-traumatic epileptogenesis.

Extracellular single-unit or multi-unit recording is a classic electrophysiological technique commonly used for measuring neuronal activity under physiological and pathological conditions *in vivo*. The activity of a single cell can be viewed as a component of a complex network and to a certain degree reflects the integrity and functional state of the neuronal network. In a previous study, Alves and associates[3] found that the mean multiple unit firing rate within 6 h after fluid percussion injury was 0.41 ± 0.01 spike/sec in rats, which was significantly less than the normal spiking rate of 2.87 ± 0.90 spikes/sec observed in sham control rats. In patients who were admitted within 12 h after severe closed head TBI, spontaneous single-unit activity was found to be 0.21 ± 0.04 spikes/sec.

Their results are consistent with our finding that the spontaneous single-unit firing rate decreased from 2.59 ± 0.18 Hz in the uninjured cortex to 1.05 ± 0.20 Hz within 1–4 h after CCI (Fig. 3,4). Because injured neurons that are silent or fire very infrequently have a lower probability of being detected with our current recording technique, the actual firing frequency in the injured cortex may be lower than what we have recorded. Further, neurons directly underneath or close to the impact site are expected to have more severe damage and thus sustain more severe loss of neuronal activity.

TBI initially causes neuronal death, excitotoxicity, deafferentation, and loss of synapses.[43,44] It appears straightforward that structural damage and neuronal death in the cortex after TBI would result in loss of synaptic input and dysfunction of the surviving neurons and lead to suppressed neuronal activity. Indeed, loss of neuronal activity is commonly observed during the acute stage after brain injuries. Studies from different models of

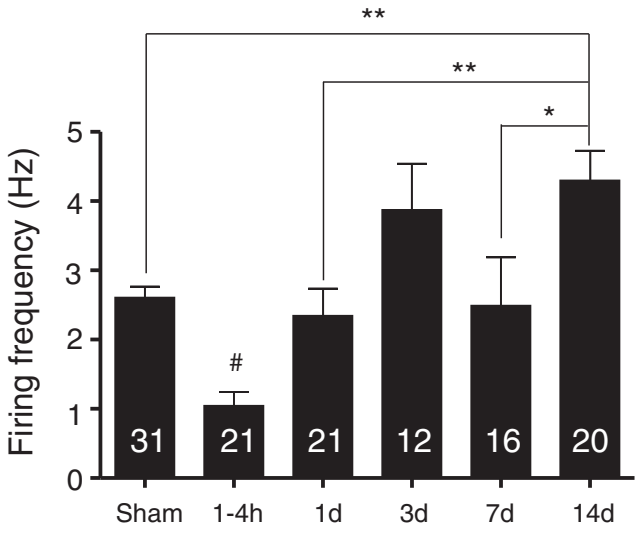

FIG. 4. Controlled cortical impact (CCI) resulted in time-dependent changes in neuronal activity in the cortical layer V pyramidal neurons in the perilesional region. The mean frequency of spontaneous single-unit activity in these neurons within 1–4 h post-CCI was significantly lower than the sham group and all other injured groups (1–4 h post-CCI group compared with all other groups, #: $p < 0.05$–0.001). The frequencies of spontaneous spikes at day 1 and day 7 post-injury were similar to that of the sham group. In contrast, the firing frequency of the 14 days post-CCI groups was significantly higher than those of the sham, 1–4 h, 1 day, and 7 day post-CCI groups (*: $p < 0.05$, **: $p < 0.01$; ***: $p < 0.001$. One-way analysis of variance followed by Newman-Keuls multiple comparison test).

brain injury indicate that both spontaneous neuronal activity and excitability are depressed in the cortex within hours to days after TBI.[1,3,4,45] In stroke models, decreases in multi-unit activity and evoked potential in the perilesion area have also been well documented.[8,46,47]

Most previous studies, however, examined changes in neuronal activity after TBI at a single time point; how and when initial loss of activity transforms into hyperactivity is not well understood. Our results indicate that cortical neuronal hyperactivity evolves from an early loss of activity and that this is not a steady process. The hypoactivity after injury recovered at 1 day and turned into hyperactivity at 3 days post-CCI. This hyperactivity recovered to normal level again at 7 days, and then became hyperexcitability again at 14 days post-CCI (Fig. 4).

A similar pattern of changes in neuronal activity *in vivo* has been reported in a middle cerebral artery occlusion model of brain ischemia in rats, in which neuronal activity was significantly reduced within the first day after injury, recovered to about normal level at 2 days post-ischemia, but reduced again at 7 days.[8] In the undercut model of brain injury in cats *in vivo*, there is an increased efficacy of excitatory connection in cortical neurons at 2 and 6 weeks after injury, but a decreased amplitude of excitatory synaptic events at 4 weeks after injury.[9]

Although the time frames among these studies are different, the results suggest that the pattern of activity changes in a period after brain injuries is time-specific and may reflect different pathological mechanisms. Thus, the first peak of hyperactivity at 2–3 days post-injury may underlie acute post-traumatic seizures while the second peak that appeared at day 14 post-CCI may result from chronic pathological events that may underlie post-traumatic epileptogenesis. Indeed, current data support that acute post-traumatic seizures are mechanistically different from chronic post-traumatic epilepsy.

The development of hyperactivity from initial hypoactivity may be attributable, at least in part, to the regulation of homeostatic synaptic plasticity. The homeostatic regulation of activity is well established in developing neurons and more recently in the adult brain.[14,48,49] A loss of neuronal activity because of sensory deprivation or injury will cause changes in neuronal intrinsic properties and synaptic transmission, leading to hyperexcitability of the affected neuronal network. In the undercut neocortex, an increase in the frequency and/or amplitude of excitatory post-synaptic currents and a decrease in inhibitory post-synaptic currents were observed and are believed to contribute to cortical hyperexcitability.[9,50] Chronically axotomized neurons also have higher input resistance and increased excitability.[9,19] Reducing neuronal activity in the normal brain for 2 or more days[13,15,16,51] is sufficient to activate homeostatic synaptic plasticity in the cortex.

In the current study, neuronal firing rate returned to normal level at 1 day post-CCI. This relatively short period of activity loss may be related to the focal injury of the CCI model, the moderate injury severity, and the recording site that was in the perilesional region. Under the condition of mild brain injury such as cortical compression, acute suppression in the amplitude of evoked sensory

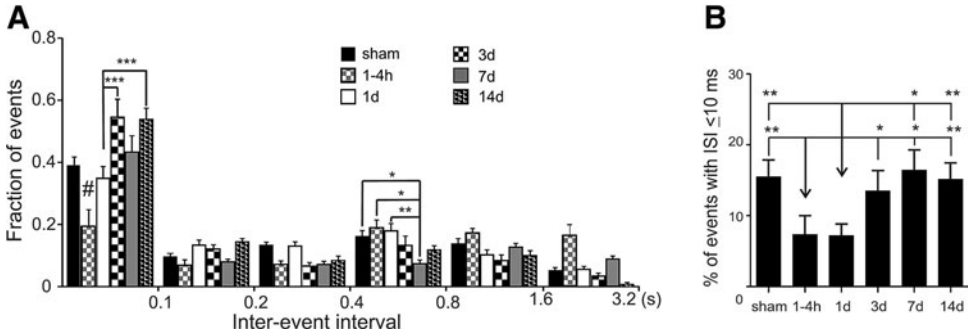

FIG. 5. (**A**) Distributions of inter-spike intervals (ISI) showed a decrease in the fraction of events with ISI ≤0.1 sec in the 1–4 h post-CCI group than all other groups (#: $p < 0.001$), and increases in the fractions of events with ISI ≤0.1 sec in 3 and 14 day groups than the 1 day group. There was also a significant decrease in the fractions of ISIs between 0.4–0.8 sec of the 7 day post-CCI group than the sham, 1–4 h, and 1 day groups. (*: $p < 0.05$, **: $p < 0.01$; ***: $p < 0.001$. Two-way analysis of variance followed by the Bonferroni *post hoc* test). (**B**) The percentages of events with ISI ≤10 msec in 1–4 h and 1 day post-CCI groups were significantly lower than almost all other groups (*: $p < 0.05$, **: $p < 0.01$. Mann-Whitney U test).

potentials occurs in the cortex, but it soon turns into hyperexcitability.[52] In more severe brain injury, such as severe TBI, the loss of activity lasts significantly longer.

A key difference between TBI and sensory deprivation condition is that TBI involves direct brain tissue damage, which is accompanied by a series of pathological events such as neuronal death, excitotoxicity, and inflammation. These factors likely also contribute to enhanced excitatory activity and amplify homeostatic/compensatory responses. Therefore, a decrease in neuronal activity seen in the current study in the CCI model and previously in the undercut model[4] likely supports the activation of homeostatic regulation of activity and contributes to the development of neuronal hyperexcitability.

As one of the major neurophysiological consequences at the early stage after TBI, loss of neuronal activity has important pathophysiological significance. On one hand, such activity loss may reflect and underlie injury-caused brain dysfunction. Promoting the recovery of activity may therefore be important for brain functional recovery after TBI. On the other hand, a quiescent period of activity after TBI may activate the homeostatic plasticity mechanism and contribute to post-traumatic epileptogenesis of the injured brain. Therefore, regulating and maintaining a relatively normal level of neuronal activity may have important significance in patients with TBI.

Acknowledgments

This research was supported by National Institutes of Health Grant NS057940, by a Project Development Team within the ICTSI NIH/NCRR Grant Number RR025761, and by the Indiana Spinal Cord and Brain Injury Research Fund from the Indiana State Department of Health (A70-0-079212 to XJ).

Author Disclosure Statement

No competing financial interests exist.

References

1. Goforth, P.B., Ren, J., Schwartz, B.S., and Satin, L.S. (2011). Excitatory synaptic transmission and network activity are depressed following mechanical injury in cortical neurons. J. Neurophysiol 105, 2350–2363.
2. Kao, C., Forbes, J.A., Jermakowicz, W.J., Sun, D.A., Davis, B., Zhu, J., Lagrange, A.H., and Konrad, P.E. (2012). Suppression of thalamocortical oscillations following traumatic brain injury in rats. J. Neurosurg. 117, 316–323.
3. Alves, O.L., Bullock, R., Clausen, T., Reinert, M., and Reeves, T.M. (2005). Concurrent monitoring of cerebral electrophysiology and metabolism after traumatic brain injury: an experimental and clinical study. J. Neurotrauma 22, 733–749.
4. Timofeev, I., Grenier, F., Bazhenov, M., Sejnowski, T.J., and Steriade, M. (2000). Origin of slow cortical oscillations in deafferented cortical slabs. Cereb. Cortex 10, 1185–1199.
5. Fischer, C., and Mutschler, V. (2002). [Traumatic brain injuries in adults: from coma to wakefulness. Neurophysiological data]. (Fre) Ann. Readapt Med Phys 45, 448–455.
6. Heiss, W.D., Hayakawa, T., and Waltz, A.G. (1976). Cortical neuronal function during ischemia. Effects of occlusion of one middle cerebral artery on single-unit activity in cats. Arch. Neurol. 33, 813–820.
7. Rosner, G., Graf, R., Kataoka, K., and Heiss, W.D. (1986). Selective functional vulnerability of cortical neurons following transient MCA-occlusion in the cat. Stroke 17, 76–82.
8. Zhang, X., Zhang, R.L., Zhang, Z.G., and Chopp, M. (2007). Measurement of neuronal activity of individual neurons after stroke in the rat using a microwire electrode array. J. Neurosci Methods 162, 91–100.
9. Avramescu, S., and Timofeev, I. (2008). Synaptic strength modulation after cortical trauma: a role in epileptogenesis. J. Neurosci. 28, 6760–6772.
10. Houweling, A.R., Bazhenov, M., Timofeev, I., Steriade, M., and Sejnowski, T.J. (2005). Homeostatic synaptic plasticity can explain post-traumatic epileptogenesis in chronically isolated neocortex. Cereb. Cortex 15, 834–845.
11. Turrigiano, G.G., Leslie, K.R., Desai, N.S., Rutherford, L.C., and Nelson, S.B. (1998). Activity-dependent scaling of quantal amplitude in neocortical neurons. Nature 391, 892–896.
12. Turrigiano, G.G. (2008). The self-tuning neuron: synaptic scaling of excitatory synapses. Cell 135, 422–435.
13. Echegoyen, J., Neu, A., Graber, K.D., and Soltesz, I. (2007). Homeostatic plasticity studied using in vivo hippocampal activity-blockade: synaptic scaling, intrinsic plasticity and age-dependence. PloS One 2, e700.
14. Keck, T., Keller, G.B., Jacobsen, R.I., Eysel, U.T., Bonhoeffer, T., and Hubener, M. (2013). Synaptic scaling and homeostatic plasticity in the mouse visual cortex in vivo. Neuron 80, 327–334.
15. Trasande, C.A., and Ramirez, J.M. (2007). Activity deprivation leads to seizures in hippocampal slice cultures: is epilepsy the consequence of homeostatic plasticity? J. Clin. Neurophysiol. 24, 154–164.
16. Bausch, S.B., He, S., Petrova, Y., Wang, X.M., and McNamara, J.O. (2006). Plasticity of both excitatory and inhibitory synapses is associated with seizures induced by removal of chronic blockade of activity in cultured hippocampus. J. Neurophysiol. 96, 2151–2167.
17. Dinocourt, C., Aungst, S., Yang, K., and Thompson, S.M. (2011). Homeostatic increase in excitability in area CA1 after Schaffer collateral transection in vivo. Epilepsia 52, 1656–1665.
18. Nita, D.A., Cisse, Y., Timofeev, I., and Steriade, M. (2006). Increased propensity to seizures after chronic cortical deafferentation in vivo. J. Neurophysiol. 95, 902–913.
19. Prince, D.A., and Tseng, G.F. (1993). Epileptogenesis in chronically injured cortex: in vitro studies. J. Neurophysiol. 69, 1276–1291.
20. Hoffman, S.N., Salin, P.A., and Prince, D.A. (1994). Chronic neocortical epileptogenesis in vitro. J. Neurophysiol. 71, 1762–1773.
21. Sharpless, S.K., and Halpern, L.M. (1962). The electrical excitability of chronically isolated cortex studied by means of permanently implanted electrodes. Electroencephalogr. Clin. Neurophysiol. 14, 244–255.
22. Guo, D., Zeng, L., Brody, D.L., and Wong, M. (2013). Rapamycin attenuates the development of posttraumatic epilepsy in a mouse model of traumatic brain injury. PloS One 8, e64078.
23. Hunt, R.F., Scheff, S.W., and Smith, B.N. (2009). Posttraumatic epilepsy after controlled cortical impact injury in mice. Exp. Neurol. 215, 243–252.
24. Bolkvadze, T., and Pitkanen, A. (2012). Development of post-traumatic epilepsy after controlled cortical impact and lateral fluid-percussion-induced brain injury in the mouse. J. Neurotrauma 29, 789–812.
25. Yang, L., Afroz, S., Michelson, H.B., Goodman, J.H., Valsamis, H.A., and Ling, D.S. (2010). Spontaneous epileptiform activity in rat neocortex after controlled cortical impact injury. J. Neurotrauma 27, 1541–1548.
26. Jin, X., Huguenard, J.R., and Prince, D.A. (2005). Impaired Cl- extrusion in layer V pyramidal neurons of chronically injured epileptogenic neocortex. J. Neurophysiol. 93, 2117–2126.
27. Jin, X., Prince, D.A., and Huguenard, J.R. (2006). Enhanced excitatory synaptic connectivity in layer v pyramidal neurons of chronically injured epileptogenic neocortex in rats. J. Neurosci. 26, 4891–4900.
28. Jin, X., Huguenard, J.R., and Prince, D.A. (2011). Reorganization of inhibitory synaptic circuits in rodent chronically injured epileptogenic neocortex. Cereb. Cortex 21, 1094–1104.
29. Munera, A., Cuestas, D.M., and Troncoso, J. (2012). Peripheral facial nerve lesions induce changes in the firing properties of primary motor cortex layer 5 pyramidal cells. Neuroscience 223, 140–151.
30. Patel, I.M., and Chapin, J.K. (1990). Ketamine effects on somatosensory cortical single neurons and on behavior in rats. Anesth. Analg. 70, 635–644.
31. Hwang, E., McNally, J.M., and Choi, J.H. (2013). Reduction in cortical gamma synchrony during depolarized state of slow wave activity in mice. Front. Syst. Neurosci. 7, 107.
32. Safaai, H., von Heimendahl, M., Sorando, J.M., Diamond, M.E., and Maravall, M. (2013). Coordinated population activity underlying texture discrimination in rat barrel cortex. J. Neurosci. 33, 5843–5855.
33. Cerri, C., Restani, L., and Caleo, M. (2010). Callosal contribution to ocular dominance in rat primary visual cortex. Eur. J. Neurosci. 32, 1163–1169.

34. Constantinidis, C., and Goldman-Rakic, P.S. (2002). Correlated discharges among putative pyramidal neurons and interneurons in the primate prefrontal cortex. J. Neurophysiol. 88, 3487–3497.
35. McCormick, D.A., Connors, B.W., Lighthall, J.W., and Prince, D.A. (1985). Comparative electrophysiology of pyramidal and sparsely spiny stellate neurons of the neocortex. J. Neurophysiol. 54, 782–806.
36. Sanabria, E.R., Su, H., and Yaari, Y. (2001). Initiation of network bursts by Ca2+-dependent intrinsic bursting in the rat pilocarpine model of temporal lobe epilepsy. J. Physiol. 532, 205–216.
37. Beck, H., and Yaari, Y. (2008). Plasticity of intrinsic neuronal properties in CNS disorders. Nature Rev. Neurosci. 9, 357–369.
38. Chagnac-Amitai, Y., Luhmann, H.J., and Prince, D.A. (1990). Burst generating and regular spiking layer 5 pyramidal neurons of rat neocortex have different morphological features. J. Comp. Neurol. 296, 598–613.
39. Agmon, A., and Connors, B.W. (1989). Repetitive burst-firing neurons in the deep layers of mouse somatosensory cortex. Neurosci. Lett. 99, 137–141.
40. Espinosa, J.S., and Stryker, M.P. (2012). Development and plasticity of the primary visual cortex. Neuron 75, 230–249.
41. Maffei, A., and Turrigiano, G. (2008). The age of plasticity: developmental regulation of synaptic plasticity in neocortical microcircuits. Prog. Brain Res. 169, 211–223.
42. Carmichael, S.T., and Chesselet, M.F. (2002). Synchronous neuronal activity is a signal for axonal sprouting after cortical lesions in the adult. J. Neurosci. 22, 6062–6070.
43. Palmer, A.M., Marion, D.W., Botscheller, M.L., Swedlow, P.E., Styren, S.D., and DeKosky, S.T. (1993). Traumatic brain injury-induced excitotoxicity assessed in a controlled cortical impact model. J. Neurochem 61, 2015–2024.
44. Reeves, T.M., Lyeth, B.G., and Povlishock, J.T. (1995). Long-term potentiation deficits and excitability changes following traumatic brain injury. Exp. Brain Res. 106, 248–256.
45. Reeves, T.M., Kao, C.Q., Phillips, L.L., Bullock, M.R., and Povlishock, J.T. (2000). Presynaptic excitability changes following traumatic brain injury in the rat. J. Neurosci. Res. 60, 370–379.
46. Neumann-Haefelin, T., and Witte, O.W. (2000). Periinfarct and remote excitability changes after transient middle cerebral artery occlusion. J. Cereb. Blood Flow Metab. 20, 45–52.
47. Moyanova, S., Kirov, R., and Kortenska, L. (2003). Multi-unit activity suppression and sensorimotor deficits after endothelin-1-induced middle cerebral artery occlusion in conscious rats. J. Neurol. Sci. 212, 59–67.
48. Turrigiano, G. (2012). Homeostatic synaptic plasticity: local and global mechanisms for stabilizing neuronal function. Cold Spring Harb. Perspect. Biol. 4, a005736.
49. Turrigiano, G. (2011). Too many cooks? Intrinsic and synaptic homeostatic mechanisms in cortical circuit refinement. Ann. Rev. Neurosci. 34, 89–103.
50. Li, H., and Prince, D.A. (2002). Synaptic activity in chronically injured, epileptogenic sensory-motor neocortex. J. Neurophysiol. 88, 2–12.
51. Maffei, A., Nelson, S.B., and Turrigiano, G.G. (2004). Selective reconfiguration of layer 4 visual cortical circuitry by visual deprivation. Nat. Neurosci. 7, 1353–1359.
52. Ding, M.C., Wang, Q., Lo, E.H., and Stanley, G.B. (2011). Cortical excitation and inhibition following focal traumatic brain injury. J. Neurosci. 31, 14085–14094.

Address correspondence to:
Xiaoming Jin, PhD
Stark Neurosciences Research Institute
Indiana University School of Medicine
320 West 15th Street, NB 500C
Indianapolis, IN 46202

E-mail: xijin@iupui.edu